NUMERICAL MODELING OF AUTOMOTIVE RIVETED CLUTCH DISC FOR CONTACT PRESSURE VERIFICATION

Samir Sfarni[1], Emmanuel Bellenger[2], Jérôme Fortin[2], Matthieu Malley[1]

[1]VALEO Transmissions Group
Product Advanced Research
Rue de Poulainville, BP 926, 80009 Amiens, France
[2]LTI EA-3899, Université de Picardie Jules Verne
IUT de l'Aisne
48 rue d'Ostende, 02100 Saint-Quentin, France

samir.sfarni@valeo.com (Samir Sfarni)

Abstract

We are interested in an automotive riveted clutch disc located in the clutch system. After gearshift and during the clutch re-engagement, the clutch disc allows to transmit a progressive torque through its axial stiffness. In order to ensure the stability of cushion curve during the lifetime of the system, we propose to perform a Finite Element model of the riveted clutch disc. The aim is to optimize the correlation between numerical and experimental results in order to obtain a prediction of contact pressures in the riveted clutch disc. This work will be the first step, leading to a framework for the drawing up of design rules for riveted clutch disc in term of stability.

1 Introduction

Car manufacturers requirements for greater power transmission, lightweight, low cost design, smaller design space, high comfort and high effectiveness lead to develop optimized clutches components. In this work we are interested in an automotive clutch system that permits the coupling and decoupling of motor and transmission during the gear change. One of the most important components used in this process is the clutch disc that allows a soft gradual re-engagement of torque transmission. This progressive re-engagement obtained by the friction disc characteristics in the axial direction preserves the driver's comfort and avoid mechanical shocks. The axial elastic stiffness of this component is obtained by a cushion disc which is a thin wavy shell, located between the two facings and fixed by rivets (Fig. 2). This axial nonlinear stiffness is obtained by cutting the cushion disc into paddles and forming them to get a wavy shape. The axial nonlinear elastic stiffness of the riveted clutch disc is described by the cushion curve. This load-deflection curve gives the axial load versus axial displacement obtained by crushing a clutch disc between two flat pressure plates. This experimental test validates a clutch disc. The objective of the present work is to model the cushion curve of the riveted assembly (cushion disc, rivets and riveted facings) in order to predict the behavior of a mounted clutch disc, decreasing the number of prototypes, experimental tests and reducing development costs. The difficulty to realize a FE model (Finite Element model) is due to the complex wavy shape of the cushion disc that generates variable contact areas during the compression phase. The elastic springback which occurs after the forming process of the cushion disc and the facings affects the geometry accuracy and alters the FE analysis results. The riveting process induces a complex response of the system. In this article, we will first detail the cushion disc FE model. Secondly, we will present the riveted clutch disc FE model. We will demonstrate that mastering the geometrical variations for the different components due to the process is of prime importance for correlating the cushion curve with experience. On another side, the high level of contact pressure applied by the cushion disc on each facing, causes it to penetrate into the facings degrading the cushion curve stability. Therefore, in order to minimize this phenomenon, we will propose a methodology for predicting contact pressures and confront it to experimental measures. This work would allow us to draw up design rules for riveted clutch discs in term of stability.

2 Clutches components

Today's passenger cars and light trucks are now almost exclusively equipped with conventional friction clutches (i.e. diaphragm spring clutches). In this work, we only consider dry friction clutches. It is composed of the clutch disc, the flywheel, and the mechanism, which is itself composed of a cover, a diaphragm spring,

and a pressure plate (Fig. 1). When the engine rotates freely (no gear engaged) no torque is transmitted because the clutch disc is not in contact with the mechanism and rotates freely (Fig. 1). When a gear is engaged, the clutch disc is compressed by the diaphragm spring between the pressure plate of the mechanism and the flywheel transmitting the rotary motion and the torque to the mechanism and thus to the wheels.

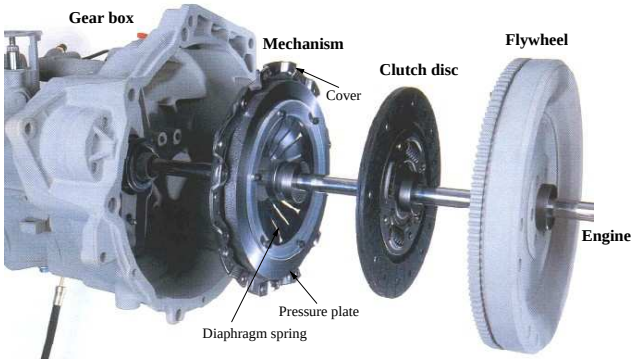

Fig. 1 View of the clutch. The clutch disc is crushed between the mechanism pressure plate and the flywheel to transmit the torque from the combustion engine to the transmission.

the necessity of coupling or decoupling the engine and transmission during gearshift induced the development of optimized clutch components that aim to transmit the torque between the pressure plate and the flywheel. In this work, we investigate the behavior of the clutch disc (Fig. 2). It allows a soft gradual re-engagement of torque transmission. This progressive re-engagement obtained by the clutch disc characteristics in the axial direction preserves the driver's comfort and avoids mechanical shocks. It also plays the role of a damper through the springs disposed around the hub. They enable the clutch disc to filter the torque variations of the combustion engine (Fig. 2).

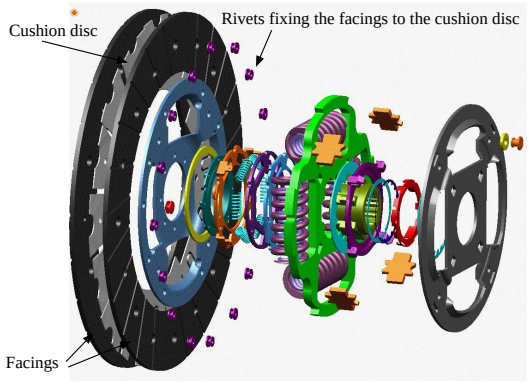

Fig. 2 Detailed design of the clutch disc.

The axial elastic stiffness of the clutch disc is obtained by a cushion disc (Fig. 3) which is a thin waved sheet, located between the two facings and fixed by rivets. It acts like a spring allowing a soft gradual re-engagement. This nonlinear axial stiffness is obtained by cutting the cushion disc into paddles and forming them to get the wavy shape (Fig. 4).

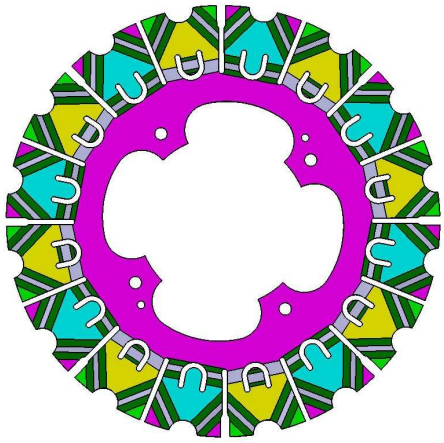

Fig. 3 Cushion disc.

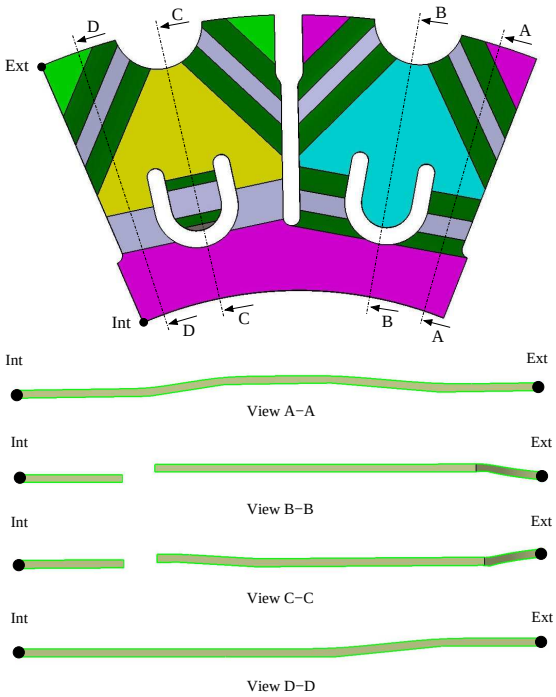

Fig. 4 Two paddles of the cushion disc with different sections.

The nonlinear axial elastic stiffness of the cushion disc is described by the cushion curve (Fig. 5). This load-deflection curve gives the axial load versus axial displacement obtained by compressing a cushion disc between two flat pressure plates. This experimental test validates a cushion disc. The wavy shape of the disc is the key element for obtaining this progressive cushion curve [1]. The cushion curve is an important technological constraint prescribed by car manufacturers. Therefore, the numerical simulation of cushion disc under ax-

ial load is particularly important for predicting its behavior in real test conditions in order to design rapidly and efficiently new clutches.

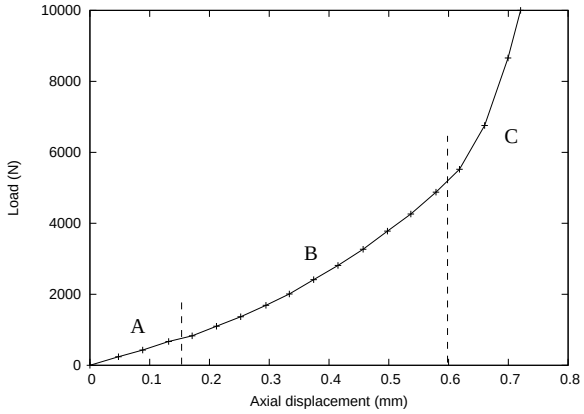

Fig. 5 Characteristic cushion curve obtained by compressing the cushion disc between two flat pressure plates. A: the pressure plate does not compress the clutch disc and the flywheel rotates independently, B: the clutch disc is partially compressed on the flywheel and partially transmits the engine torque, C: the clutch disc completely transmits the engine torque.

It is required to master the cushion disc before investigating the nonlinear axial elastic stiffness of the cushion disc riveted between the two facings of the clutch disc. Therefore, in the first part of this article, we will present the the cushion disc FE model used to simulate the cushion curve. We will then discuss the correlation observed between experimental and numerical results. After validating the FE model robustness, we will study the influence of geometrical parameters by a numerical Design Of Experiments (DOE). We will identify the most influent geometrical parameters and measure them to correct the theoretical geometry of the cushion disc used for computations.

3 Cushion disc FE model for the cushion curve computation

The difficulty to implement a FE model for the prediction of cushion curves is due to the complex wavy shape of the thin cushion disc that generates variable contact areas during the compression phase. Furthermore, the elastic springback which occurs after the forming process of the cushion disc affects the geometry accuracy. Besides, the cushion disc geometry is difficult to control with conventional metrological tools because it bends under the load applied by any mechanical probe. All this influences the accuracy and repeatability of experimental correlation with FE models.

A FE model was implemented by applying ANSYS Parametric Design Language (APDL). Only two paddles of the cushion disc are modeled taking into account the symmetry. The cushion disc (Fig. 6) is meshed with shell elements (Shell 181 in the ANSYS library) according to its thin thickness ($0.7\,mm$) and computed using a linear elastic material law. The pressure plates are modeled by two flat rigid plates that compress the disc axially to simulate its behavior during the gear re-engagement. A master-slave surface to surface contact pair is used between the cushion disc (master surface) and each pressure plate (slave surfaces). The contact elements associated to master and slave surfaces are respectively Contact 173 and Target 170 in the ANSYS library. In this work, we have used an Augmented Lagrangian Method (ALM) to solve the contact problem [2]. One of the two plates is fixed in all the directions but the second one moves axially compressing the disc up to 70% of its height. The plate motion is controlled by displacement instead of force in order to limit convergence problems. Only tangential displacement and rotation towards the z axis were blocked on the internal ring of the disc in order to avoid rigid body motion, the other directions are let free according to the experimental test. Symmetry boundary conditions were applied on both sides of the disc (Fig. 6).

Firstly, we compute a cushion curve by assuming a perfect concordance of the geometry between the designed and the manufactured cushion disc. The result shows a difference with experimental results (Fig. 7). This gap could be caused by two major factors:

1- An inadequate modeling by the FEM which can result from the choice of numerical parameters such as: symmetry conditions, contact parameters, convergence parameters or mesh density.

2- An inadequate cushion disc geometry description that could vary in reality due to the process.

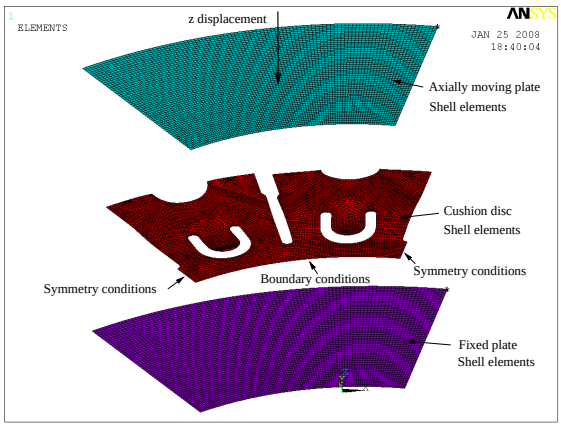

Fig. 6 Cushion disc Finite Element model.

Firstly, a sensitivity study was performed on numerical parameters. None of these investigations was able to explain the observed difference between the computed and the experimental cushion curve (Fig. 7) [1]. This led us to study the influence of the cushion disc geometry on the computed cushion curve. For this, a numerical Design Of Experiments (DOE) has been performed to determine the most influent geometrical factors on

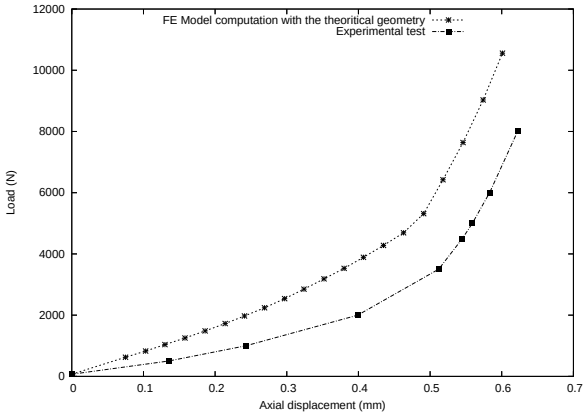

Fig. 7 Cushion curve correlation with the FE model using theoretical geometry.

the cushion curve, with the aim to measure them and to correct the cushion disc geometry.

4 Numerical Design Of Experiments

A numerical DOE has been performed to study the influence of geometrical parameters selected in regard to their supposed influence on the cushion curve. A parametric cushion disc CAD model has been generated using CATIA V5 software. It allows us to modify easily the geometrical characteristic of the cushion disc. The selected parameters (or factors) are the global disc height A, its thickness C, the radii of fillets B, and the bending line width D which is the perpendicular distance between two bending lines (Fig. 8). All these parameters are specified during the design process, excepted the fillets radii which are a free process results. These factors can anyway have a certain variability that is supposed to be the cause of our correlation gap. When geometrical parameters values are uncertain, the "one factor a time" method is commonly used to investigate the effects of parameters variations. However, it does not take into account the possibility of interactions among parameters. The low number of selected factors allows us to use a numerical DOE with the full factorial method. It permits the analysis of relative importance of each parameter and identifies any interactions among them. Four parameters with two levels (Tab. 1) have been selected for this study. For factor A, the nominal value is $0.95\,mm$. We expect it to be less than specified after the forming process because of the springback effect. So we have chosen to set the superior value equal to the nominal one. The fillets radii B are a free consequence of the process. It is set to $30\,mm$ for nominal FE calculations and we have chosen to set inferior and superior levels to $20\,mm$ and $50\,mm$ respectively, in accordance with the usually measured values. The thickness levels C are based on its upper and lower tolerances and the bending line width levels D are set to a reasonable variation around the nominal value. The DOE table is shown in Tab. 2. It represents $2^4 = 16$ cushion curves FE simulations.

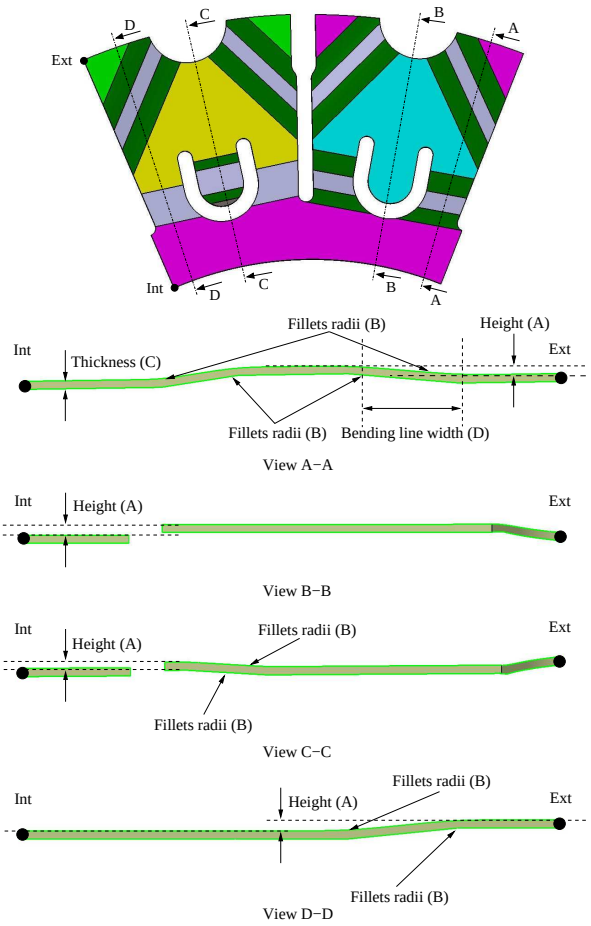

Fig. 8 Selected factors for the numerical design of experiments.

Tab. 1 Factor levels.

	Inferior level (-)	Superior level (+)	Nominal values
A: Global disc height	0.85 mm	0.95 mm	0.95 mm
B: Fillets radii	20 mm	50 mm	30 mm
C: Thickness	0.65 mm	0.75 mm	0.7 mm
D: Bending line width	6 mm	8 mm	7 mm

Tab. 2 Calculations performed for the numerical Design of Experiments.

	A	B	C	D		A	B	C	D
1	-	-	-	-	9	-	-	-	+
2	+	-	-	-	10	+	-	-	+
3	-	+	-	-	11	-	+	-	+
4	+	+	-	-	12	+	+	-	+
5	-	-	+	-	13	-	-	+	+
6	+	-	+	-	14	+	-	+	+
7	-	+	+	-	15	-	+	+	+
8	+	+	+	-	16	+	+	+	+

A total of 16 cushion curves FE simulations have been performed [3]. Their results are presented in Fig. 9. The range of variation of these 16 models confirms the importance of geometry. From the study of the influence of each factor on displacement at 100%, 50%, 25% of the nominal load (fixed here at 8000 N) and also on the shape coefficient, which represents the ratio of displacements d100%/d25%, we can deduce a significant predominance of the factors B and C (fillets radii and disc thickness respectively), particularly at 25% and 50% of the nominal load. The same remark can be done for the shape coefficient. The disc height A is influent at 100% of the nominal load and finally, the factor D (bending line width) seems to be of a second order. From the study of the diagrams of influence of the four factors and their interactions on the shape coefficient and at 100% of the nominal load we can conclude that the only influent interaction on the shape coefficient is between factors B and C. This because a variation of thickness induces a variation of fillet radii, but the opposite is not true. Interaction between factors B and D is influent on 100% of the nominal load and on the shape coefficient. A variation of the bending line width implies certainly a variation of the fillets radii, (the opposite is not true). Finally, factors B and C are the most influent on all parts of the curve and factor A (disc height) is influent on its top (nominal load).

The numerical DOE confirms the influence of the cushion disc geometry on the computed cushion curves. Even though the results show a predominance of the parameters B and C, for a better accuracy, all the geometrical factors studied above have been measured with the aim to be introduced in a corrected CAD model of the cushion disc for comparison with experimental results.

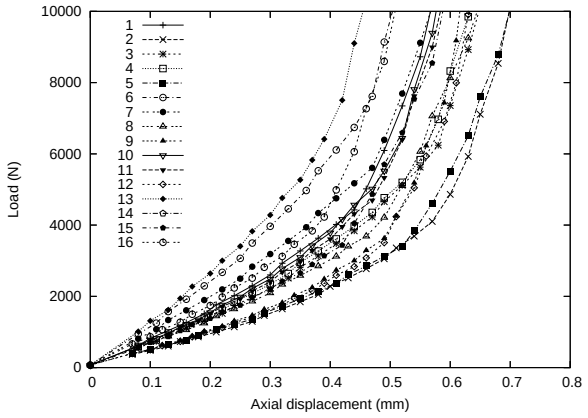

Fig. 9 Cushion Curves obtained with the design of experiments.

4.1 Geometry corrections of the cushion disc

Two cushion discs of the same reference have been measured with two different methods. The first one using a Mitutoyo Quick Vision system after two paddles have been cut and observed on the profile view. The second one is a disc of the same reference (same theoretical geometry). It has been measured using a Mitutoyo laser probe that generates a cloud of points representing the disc surface. For the first disc, measured with the metrological camera, we have found a global height A value of $0.9\,mm$ (instead of $0.95\,mm$ specified in the theoretical geometry). The fillet radii B (the most important factor) has been measured on the two paddles using the same metrological camera. Results of the measures are given in Tab. 3. The thickness C has been also measured using the same camera, by observing the disc profile side. A value of $0.662\,mm$ was found. The second disc, whose surface was discretized using a laser probe has been post treated by importing the point cloud in a CAD software (CATIA V5). We have thus found a global height A of $0.83\,mm$ and the corresponding fillets radii given in Tab. 3. A thickness C of $0.68\,mm$ has been measured using a Palmer tool.

Tab. 3 Measured fillets radii.

	First cushion disc (metrological camera)	Second cushion disc (laser probe)
R1	39.2 mm	30.7 mm
R2	64 mm	61.2 mm
R3	44.8 mm	47.4 mm
R4	31 mm	59 mm
R5	55.3 mm	34 mm
R6	63.8 mm	58.7 mm

The measured factors A, B and C have been all introduced in the CATIA V5 geometry of the cushion disc and a FE model has been carried out introducing the corrected geometry for the two measured discs. For the first disc (measured with a metrological camera), the computation with corrected geometry (parameters A, B and C corrected) gives a much better agreement with experimental results. For the second disc (laser probe measurement), the comparison shows a better agreement in the curve shape but a poor correlation of the displacement values obtained, particularly at the top of the curve. The above mentioned observation could be explained by the flatness defaults of the disc which can cause a global translation of the curve to the right. Indeed, if two symmetric points of the disc are not in contact with the flat plate at the same time, this could result in a non loaded displacement, translating the curve to the right. The cushion curve measurement machine gives a value of flatness default corresponding to the maximal difference measured by two of the three displacement sensors disposed around the upper pressure plate compressing the cushion disc. In the case of the first disc, the average flatness default measured was $0.0412\,mm$, while it was $0.0862\,mm$ for the second one. This tends to show that the experimental curve of the second disc is more influenced by flatness defaults. A solution for minimizing the flatness defaults, for a better comparison between experimental and numerical curves, consists in taking the nominal load ($8000\,N$) as reference, corresponding to the zero displacement. It is assumed that the value of displacement measured at $8000\,N$ is much less influenced by flatness defaults, than the one measured at a low load. Fig. 10 shows

the previous experimental, standard geometry, and corrected geometry calculation curves, compared by taking the zero displacement at 8000 N. No any additional calculation was needed for this comparison, a simple x-axis translation is needed. For both discs, comparisons taking the nominal load as reference show a great correlation between experimental tests and numerical results for the corrected geometry.

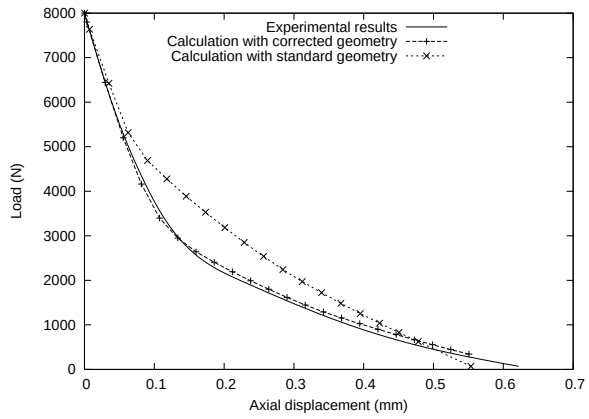

(a)

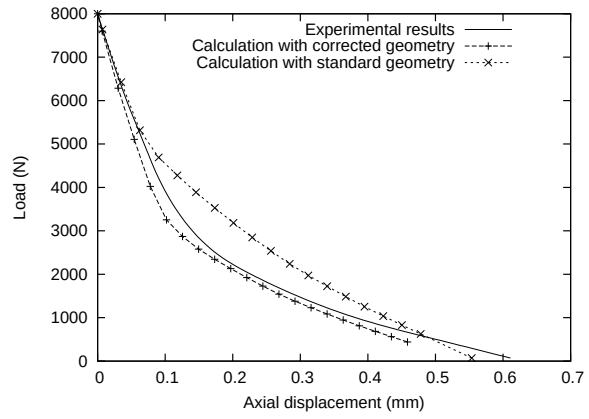

(b)

Fig. 10 Cushion curve correlation by taking the nominal load as reference: (a) First cushion disc (metrological camera measurement), (b) Second cushion disc (laser probe measurement).

The above presented work allows us to conclude that geometrical parameters and flatness defaults were the most important factors influencing our results, and the root cause of the difference between experience and calculation. The remaining difference between the two cushion curves can be caused by the measurement method of the fillets and the average values introduced. Moreover, we have only measured two paddles and supposed all the others to be similar, while in reality, some paddles could have a different geometry (inducing a different stiffness). The disc thickness can also slightly vary on two different points of a disc, causing slight stiffness variations between different paddles. The cushion curve measurement can also introduce some variability through the measuring machine and the way the disc is disposed on it.

The parametric model study allowed us to confirm the robustness of the FE model. A FE Design Of Experiments was then carried out to identify the most influent geometrical parameters. This led us to measure the fillets radii, thickness and global height of the disc. Once these parameters introduced in the theoretical geometry, we could observe a greater concordance between calculation and experience. It was necessary to compare the experimental and calculated curves by eliminating the flatness defaults to obtain a great concordance for both discs studied. We can thus conclude that a good characterization of only three important geometrical parameters and a comparison of curves starting by the nominal load at zero displacement is sufficient for a good prediction of cushion curves. The next step will be the modeling of a riveted clutch disc including the facings that influence the cushion curve of the clutch disc, probably by a combination of the cushion disc and facing deformations due to the riveting process.

5 Riveted clutch disc FE model for the cushion curve computation

The objective is to model the cushion curve of the riveted assembly (cushion disc, rivets and riveted facings) in order to predict the behavior of a mounted riveted clutch disc. As seen above, the difficulty to realize a FE Model is due to the complex wavy shape of the cushion disc. For the riveted clutch disc, the elastic springback which occurs after the forming process of the cushion disc and the facings affects the geometry accuracy and alters the FE analysis results. The riveting process induces a complex response of the system, affected by clamping force, clearance, geometry defaults and other phenomena.

A FE model was implemented by applying ANSYS Parametric Design Language (APDL). Only two half paddles of the cushion disc are modeled taking into account the symmetry. The FE model is made up of the cushion disc, two half rivets, two facings and two flat rigid plates (Fig. 11). The cushion disc is meshed with shell elements (Shell 181 in the ANSYS library) according to its thin thickness (0.7 mm), the rivets and the facings are meshed with solid cubic elements (Solid 45 in the ANSYS library). The model is computed using a linear elastic material law. Ten master-slave surface to surface contact pairs are used in the model. Two pairs are used between the cushion disc and each facing, the facings and the flat rigid plates, the cushion disc and the rivets heads, the rivets shanks and the facings, the rivets heads and the facings respectively. The contact elements associated to master and slave surfaces are respectively Contact 173 and Target 170 in the ANSYS library. One of the two plates is fixed in all the directions but the second one moves axially compressing the disc up to 70% of its height. The FE model is run in three load steps: successive simulations of both rivets pre-load due to applied torque (Pret179 in the ANSYS library) and computation of the cushion curve by compressing the riveted clutch disc between two pressure plates.

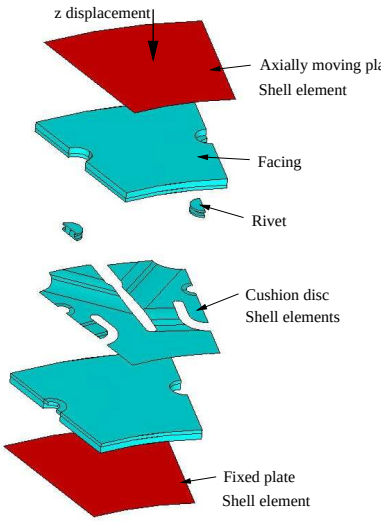

Fig. 11 Riveted disc Finite Element model.

Firstly, we compute the cushion curve of the riveted disc with the corrected geometry of the cushion disc defined above. The result show a difference with the experimental result (Fig. 12) As seen above for the study of the cushion disc, this gap could be caused by two major factors:

1- An inadequate modeling by the FEM which can result from the choice of numerical parameters such as: symmetry conditions, contact parameters, convergence parameters, mesh density, riveting clearance or clamping force [4].

2- An inadequate rivets and facings geometry description that could vary in reality due to the process.

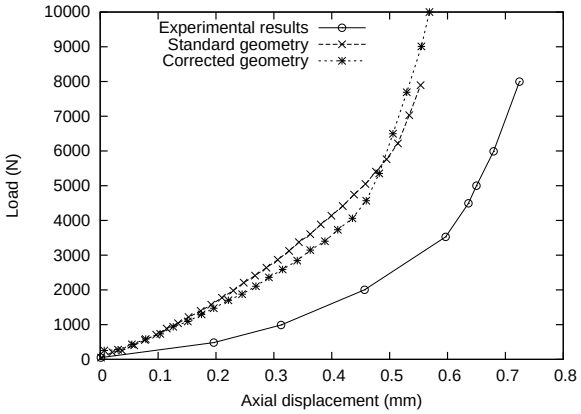

Fig. 12 Cushion curves of the riveted clutch disc with corrected and theoretical geometries of the cushion disc.

Therefore, a sensitivity study was performed on numerical parameters such as the contact stiffness, the penetration tolerance, the friction coefficient, the material properties, the riveting clearance and the clamping force. We have also studied the geometrical variation influence of facings and rivets with their combination. None of these investigations were able to explain the observed difference between the computed and the experimental cushion curve except an inadequate facing geometry that could also vary due to the production process. This led us to study the influence of the facings geometry on the computed cushion curve.

5.1 Geometry corrections of the facings

To quantify the influence of the facings geometry on the cushion curve of the riveted clutch disc, the facings flatness defaults have been measured. The measurement of the facings flatness defaults gives values up to 0.8 mm. In order to introduce the facings flatness defaults in the CATIA V5 geometry of the riveted clutch disc, several types of geometrical facings defaults have been tested. The different types of defaults tested are in accordance with the deformations of facings gathered on the production line. Thus, mid-radius bending, conical, circumferential undulation and double circumferential undulation defaults have been introduced in the riveted clutch disc model (Fig. 13). From these calculations with the corrected cushion disc and facings geometries introduced in the previous FE model, we can conclude that a double circumferential undulation defaults with two different heights of 0.07 mm and 0.01 mm enables to obtain a great improvement of the cushion curve by taking into account the flatness defaults of the facings (Fig. 14). As seen above, these curves are given by taking the zero displacement at 8000 N.

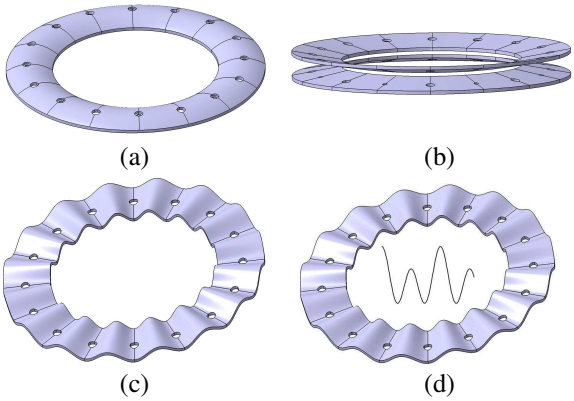

Fig. 13 Geometrical facings defaults: (a) mid radius bending, (b) conical, (c) circumferential undulation, (d) double circumferential undulation.

The above presented work allows us to conclude that a good prediction of the cushion curve of a riveted clutch disc should be done by correcting the cushion disc and facings geometries. A good characterization of only three important geometrical parameters of the cushion disc, the introduction of a double circumferential undulation default of the facings and a comparison of curves starting by the nominal load at zero displacement are sufficient for a good prediction of cushion curves.

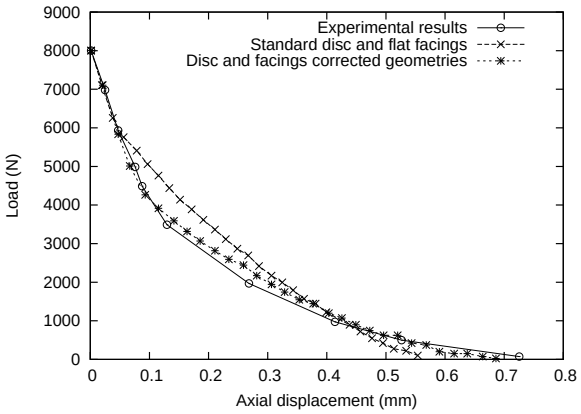

Fig. 14 Cushion curve correlation between corrected corrected geometries and standard models.

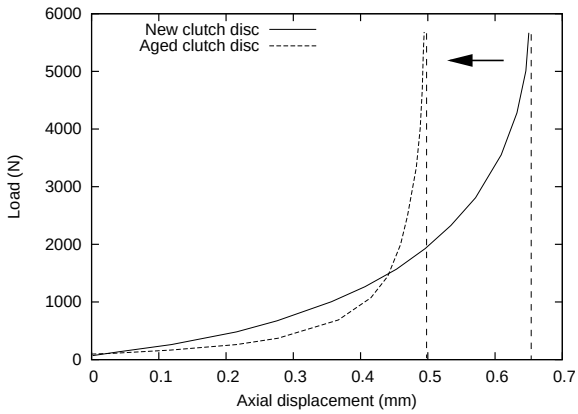

Fig. 16 Degradation of the cushion curve during the lifetime of the riveted clutch disc.

6 Contact pressure analysis

The prediction of the cushion curve presented above is valid for a new riveted clutch disc at the beginning of its lifetime. Indeed, the high level of contact pressure applied by the cushion disc on each facing during the lifetime of the riveted clutch disc leads to an embedding phenomenon between the facings an the cushion disc (Fig. 15). The cushion disc penetrates into the facings, wearing them and degrading the cushion curve stability (Fig. 16). This phenomenon degrades the driver's comfort. In order to control this phenomenon, the estimation of the contact pressures for a designed clutch disc is of prime importance. In a first step, the aim of this work is not to simulate the complex evolution of the cushion curve during its lifetime by taking into account the embedding phenomenon and other. We propose to verify if the riveted clutch disc FE model defined above, enables the contact pressures to be compared with experimental results at the beginning of the clutch disc lifetime. This work would allow us to establish design rules for riveted clutch discs in term of stability.

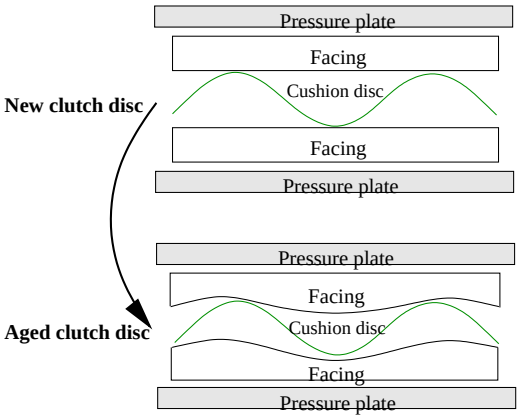

Fig. 15 Embedding phenomenon.

In this work, we propose a comparison between the values of contact pressures obtained with a FE model and with a commercial pressure-sensitive film (Fuji Prescale) which is employed in industrial and lab applications to evaluate contact pressures [5]. This film consists of a layer of liquid filled bubbles interposed between two paper sheets: as the applied pressure increases, more bubbles are broken, thus producing a red stain whose intensity is related to the contact pressure. Fig. 17 shows a comparison between the calculated and the measured contact pressures distributions defined on the pressure plate side of a facing. We can see that the distribution of the calculated contact pressures is in good agreement with the measured one. Fig. 18 shows the evolution of the contact pressure along the framed contact line defined in Fig. 17. The x-axis corresponds to the location on the chosen contact area. Analysis of the Fuji Film stains was performed using a digital imaging software [6]. Fig. 18 shows a good correlation between numerical and experimental contact pressures.

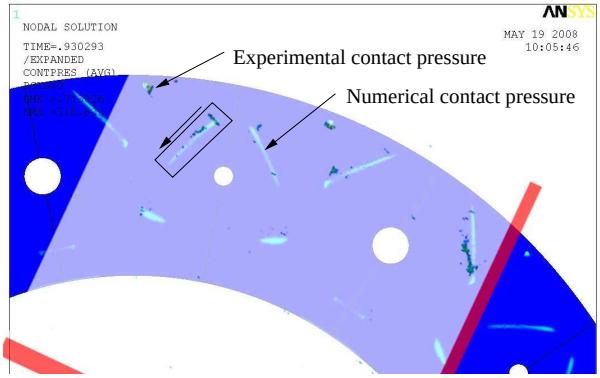

Fig. 17 Comparison between the calculated and the measured contact pressures distributions (pressure plate side).

Fig. 19 shows a comparison between the calculated and the measured contact pressures distributions defined on the pressure flywheel side of a facing. We can see that

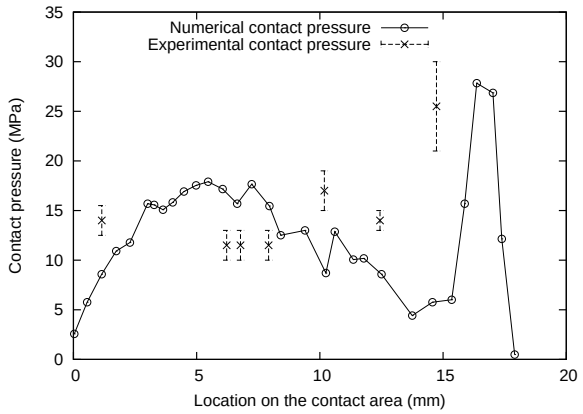

Fig. 18 Contact pressure correlation between numerical and experimental results (pressure plate side).

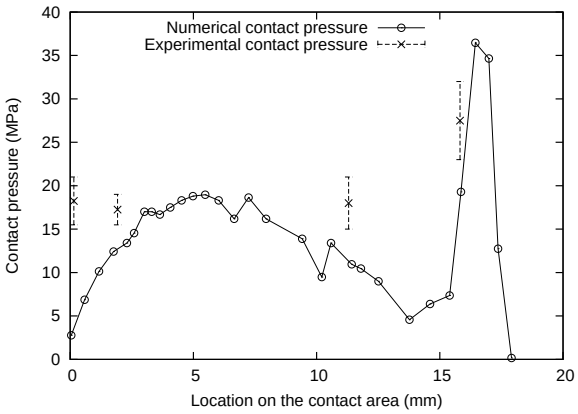

Fig. 20 Contact pressure correlation between numerical and experimental results.

the distribution of the calculated contact pressures is in good agreement with the measured one. Fig. 20 shows the evolution of the contact pressure along the framed contact line defined in Fig. 19. The x-axis corresponds to the location on the chosen contact area. Analysis of the Fuji Film stains was performed using a digital imaging software. Fig. 20 shows a good correlation between numerical and experimental contact pressures.

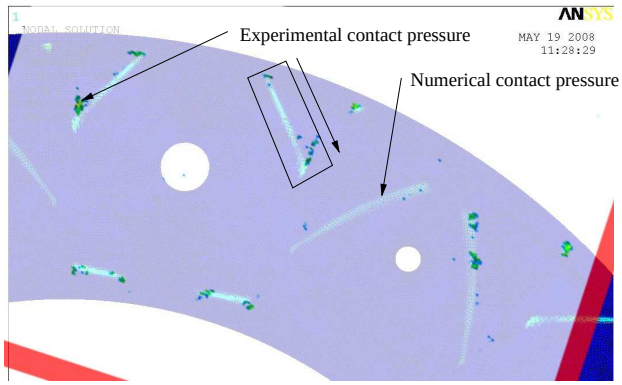

Fig. 19 Comparison between the calculated and the measured contact pressures distributions (flywheel side).

The results presented above, concerning the correlation of contact pressures in the riveted clutch disc at the beginning of its lifetime have confirmed the robustness of the proposed method. Therefore, the next step will be to establish design rules for riveted clutch discs in term of stability by avoiding the embedding phenomenon.

7 conclusion

The cushion curve is an important technological constraint prescribed by car manufacturers. Therefore, the numerical simulation of riveted clutch disc under axial load is particularly important for predicting its behavior in real test conditions in order to design rapidly and efficiently new clutches. To reach this goal, it was required to master the cushion disc before investigating the nonlinear axial elastic stiffness of the cushion disc riveted between the two facings of the clutch disc. Therefore, in the first part of this article, we have presented the FE model used to simulate the cushion disc. A FE Design Of Experiments was then carried out to identify the most influent geometrical parameters. We have concluded that a good characterization of only three important geometrical parameters and a comparison of curves starting by the nominal load at zero displacement is sufficient for a good prediction of cushion curves. The next step was the modeling of a riveted clutch disc including the facings that influence the cushion curve of the clutch disc. The above presented work allowed us to conclude that a good prediction of the cushion curve of a riveted clutch disc should be done by correcting the cushion disc and facings geometries. The introduction of a double circumferential undulation default of the facings and a comparison of curves starting by the nominal load at zero displacement are sufficient for a good prediction of cushion curves. In order to avoid the embedding phenomenon which degrades the cushion curve stability and the driver's comfort, we have verified that the riveted clutch disc FE model enables the contact pressures to be compared with experimental results. Therefore, this work is the first step leading to a framework for the drawing up of design rules for riveted clutch discs in term of stability.

8 References

[1] S. Sfarni, E. Bellenger, J. Fortin, P. Hervet, and M. Malley. Finite element analysis of cushion discs in automotive clutches. In *21st JUMV International Automotive Conference with Exhibition*, Belgrade, Serbia, April 2007. University of Belgrade, Faculty of Mechanical Engineering.

[2] J. C. Simo and T. A. Laursen. An augmented lagrangian treatment of contact problems including friction. *Computers and Srtuctures*, 42:527–634, 1992.

[3] S. Sfarni, E. Bellenger, J. Fortin, and M. Malley. Finite element analysis of automotive cushion discs. *Thin-Walled Structures*, In press, 2008.

[4] M.A. McCarthy, V.P. Lawlor, W.F. Stanley, and C.T. McCarthy. Bolt-hole clearance effects and strength criteria in single-bolt, single-lap, composite bolted joints. *Composites Science and Technology*, 62:14151431, 2002.

[5] R.J. Singerman, D.R. Pedersen, and T.D. Brown. Quantitation of pressure-sensitive film using digital image scanning. *Experimental Mechanics*, 44:99105, 1987.

[6] K. N. Bachus, A. L. DeMarcoa, K. T., D. S. Horwitz, and D. S. Brodke. Measuring contact area, force, and pressure for bioengineering applications: Using fuji film and tekscan systems. *Medical Engineering and Physics*, 28:483488, 2006.